ACI STRUCTURAL JOURNAL TECHNICAL PAPER

Title no. 105-S10

Residual Seismic Performance of Reinforced Concrete Bridge Piers After Moderate Earthquakes

by Young-Soo Chung, Chang Kyu Park, and Christian Meyer

An experimental investigation was conducted to evaluate the seismic ductility of previously damaged concrete columns. Eight circular concrete columns 600 mm (23.6 in.) in diameter and 1500 mm (59.0 in.) in height were constructed with three test parameters: confinement ratio, lap-splice of longitudinal steel, and retrofitting fiber-reinforced polymer (FRP) materials. The objective of this research was to subject reinforced concrete (RC) bridge piers to artificial earthquake motions using a pseudo-dynamic test (PDT), and then to examine their seismic performance in a quasi-static test (QST). The seismic enhancement of FRP wraps was also investigated. Six specimens were loaded to induce damage by a series of four artificial earthquakes, which were developed by the Korea Highway Corporation (KHC), to be representative of earthquakes in the Korean peninsula. Following the PDT, the six predamaged specimens were subjected to inelastic cyclic loading while under a constant axial load of 10% of the column axial capacity. Two reference specimens without predamage were subjected to similar quasi-static loads.

Test results showed that all specimens behaved almost linearly under moderate artificial earthquakes (PDT). Except for the ordinary specimens with lap-spliced longitudinal bars, most specimens predamaged during the PDT generally demonstrated good residual seismic performance. The predamage introduced during the PDT in ordinary specimens lowered their seismic performance. RC bridge specimens retrofitted with fiber composite wraps in the potential plastic hinge region exhibited enhanced flexural ductility.

Keywords: fiber-reinforced concrete; lap splice; pier; reinforced concrete; seismic; transverse confinement.

INTRODUCTION

Until recently, Korea was considered to be immune from earthquake hazards because it is located relatively far away from active faults. It has been observed in the Korean peninsula, however, that the number of low and moderate earthquakes has increased year by year. Recent earthquakes in Turkey (1999), Taiwan (1999), India (2001), Sumatra (2004), and Fukuoka (2005) have caused considerable loss of life and extensive damage to structures. It is particularly noteworthy that the Turkey (1999) and Taiwan (1999) earthquakes are similar in scale, but the damage in Turkey was typically more severe because of the lower seismic preparedness. Hence, to protect human life and property from seismic hazard even in countries of moderate seismicity, assuring seismic safety of various infrastructures is very important. The collapse or near collapse of bridge structures during the 1994 Northridge earthquake and the 1995 Hyogoken Nambu earthquake were noted with concern in Korea and prompted safety evaluations of various structures that were or were not designed to resist earthquakes.

Reinforced concrete (RC) bridges are potentially among the most seismically vulnerable structures. The damage of RC columns in regions that experience inelastic action depends on the characteristics of the earthquakes as well as column details. The extent of this damage affects the bridge performance during the design-level earthquake and the feasibility of restoring the columns to their preearthquake conditions. The research reported herein has focused on the repair and strengthening of shear dominated RC columns that were damaged by minor or moderate earthquakes. Moreover, for practical reasons, lap splices of longitudinal bars were used in the plastic hinge region of most RC bridge columns that were constructed before the seismic design code of the Korea highway bridge design specification (KHBDS) was implemented in 1992. Therefore, the purpose of the research presented herein was to investigate the effect of lap splices of longitudinal reinforcement on the seismic performance of RC bridge piers and to evaluate the residual seismic performance of such piers with prior earthquake damage. The last objective of this investigation was to develop an efficient strengthening method for RC piers that were built with lap-spliced longitudinal bars.

It is known that closely spaced transverse reinforcement in the potential plastic hinge zone of bridge columns increases the ultimate strength and strain capacity of the concrete core. Chai et al.[1] reported that the use of steel jacketing to retrofit columns was effective in restoring the flexural strength and the ductility of a damaged column that had suffered total bond failure of reinforcement spliced in the plastic hinge region. Saadatmanesh et al.[2] experimentally studied the seismic behavior of RC columns strengthened with fiber reinforced plastic composite straps and showed that such straps were very effective in confining the core concrete and preventing the longitudinal bars from buckling under cyclic loading. They also conducted an experimental investigation into the flexural behavior of four earthquake-damaged RC columns repaired with prefabricated fiber-reinforced plastic wraps and verified the effectiveness of the proposed repair technique by showing that the flexural strength and displacement ductility of the repaired columns were higher than those of the original column. Aboutaha et al.[3] have also reported the effects of confinement on the compressive strength and ductility of RC bridge piers. They investigated the effect of lap splice lengths of the longitudinal bars and the repair of lap splice failures in damaged concrete columns. A total of six specimens with a 457.2 x 914.4 mm (18.0 x 36.0 in.) cross section were fabricated and tested under axial load and cyclic lateral displacement to examine the effect of two confinement steel types and different repair

ACI Structural Journal, V. 105, No. 1, January-February 2008.
MS No. S-2006-380.R2 received November 16, 2006, and reviewed under Institute publication policies. Copyright © 2008, American Concrete Institute. All rights reserved, including the making of copies unless permission is obtained from the copyright proprietors. Pertinent discussion including author's closure, if any, will be published in the November-December 2008 *ACI Structural Journal* if the discussion is received by July 1, 2008.

ACI member **Young-Soo Chung** *is a Professor in the Department of Civil Engineering, Chung-Ang University, Seoul, South Korea. He received his PhD from Columbia University, New York, NY, in 1988. His research interests include seismic analysis and design of reinforced concrete structures, especially concrete bridge structures, concrete structural design code, repair and retrofit of concrete, damage assessment, and reliability.*

Chang Kyu Park *is an Engineer at Hyundai Engineering and Construction Co., LTD, Seoul. He received his BS, MS, and PhD from Chung-Ang University in 1997, 2001, and 2005, respectively. His research interests include seismic design and analysis of reinforced concrete structures and the repair and retrofit of concrete structures.*

Christian Meyer, *FACI, is a Professor and Chairman of the Department of Civil Engineering and Engineering Mechanics at Columbia University. He is Chair of ACI Committee 555, Concrete with Recycled Materials, and a member of ACI Committees 446, Fracture Mechanics; 544, Fiber Reinforced Concrete; E803, Faculty Network Coordinating Committee; Joint ACI-ASCE Committee 447, Finite Element Analysis of Concrete Structures; and the ACI Board Advisory Committee on Sustainability. His research interests include concrete materials science and technology and the use of recycled materials.*

methods. Results from the cyclic lateral load test showed that the retrofitted columns reached their design strength and had good shear strength and ductility. Lehman et al.[4] experimentally investigated the performance of earthquake-damaged RC columns repaired by different techniques, depending on the damage level and details of the original columns: headed reinforcement, mechanical couplers, and cover concrete patching with epoxy injection. The effectiveness of each repair technique was determined by comparing responses of the repaired columns and original column with the design requirements.

The goal of the present study was to induce damage in RC bridge piers with lap-spliced longitudinal bars in the plastic hinge region using artificial earthquake motions with specified peak ground accelerations (PGAs)[5] in a pseudo-dynamic test (PDT) and to examine the residual seismic performance of these damaged specimens in a quasi-static test (QST). Finally, the effect of fiber-reinforced polymer (FRP) wraps to improve the performance of such RC bridge piers with lap-spliced longitudinal bars was investigated. Eight circular test specimens with an aspect ratio of 2.5 were constructed. The three test parameters were: transverse confinement, lap splice of longitudinal steel, and retrofitting FRP materials. To provide different confinement levels, test specimens were designed in accordance with either ordinary, intermediate, or seismic design concepts. Because longitudinal bars in RC bridge piers are often lap spliced for ease of construction, four test specimens were made with 50% of the longitudinal reinforcement spliced. Six columns were damaged in the PDT and then subjected to lateral inelastic cyclic loadings (QST) while under a constant axial load of 10% of the column axial capacity. Because the residual seismic performance of RC bridge piers after exposure to low or moderate earthquakes is very important,[6-8] damage was induced with simulated seismic ground motions that are likely to occur in the Korean peninsula. The effect of lap splice, retrofit technique, and transverse confinement on the flexure/shear-critical RC columns was investigated. The residual seismic performance of the damaged test specimens was evaluated by measuring displacements, curvatures, and energy absorption.

RESEARCH SIGNIFICANCE

The objective of the research reported herein was to investigate the residual seismic performance of earthquake-damaged RC bridge piers that were constructed before or after the implementation of a seismic design code in Korea

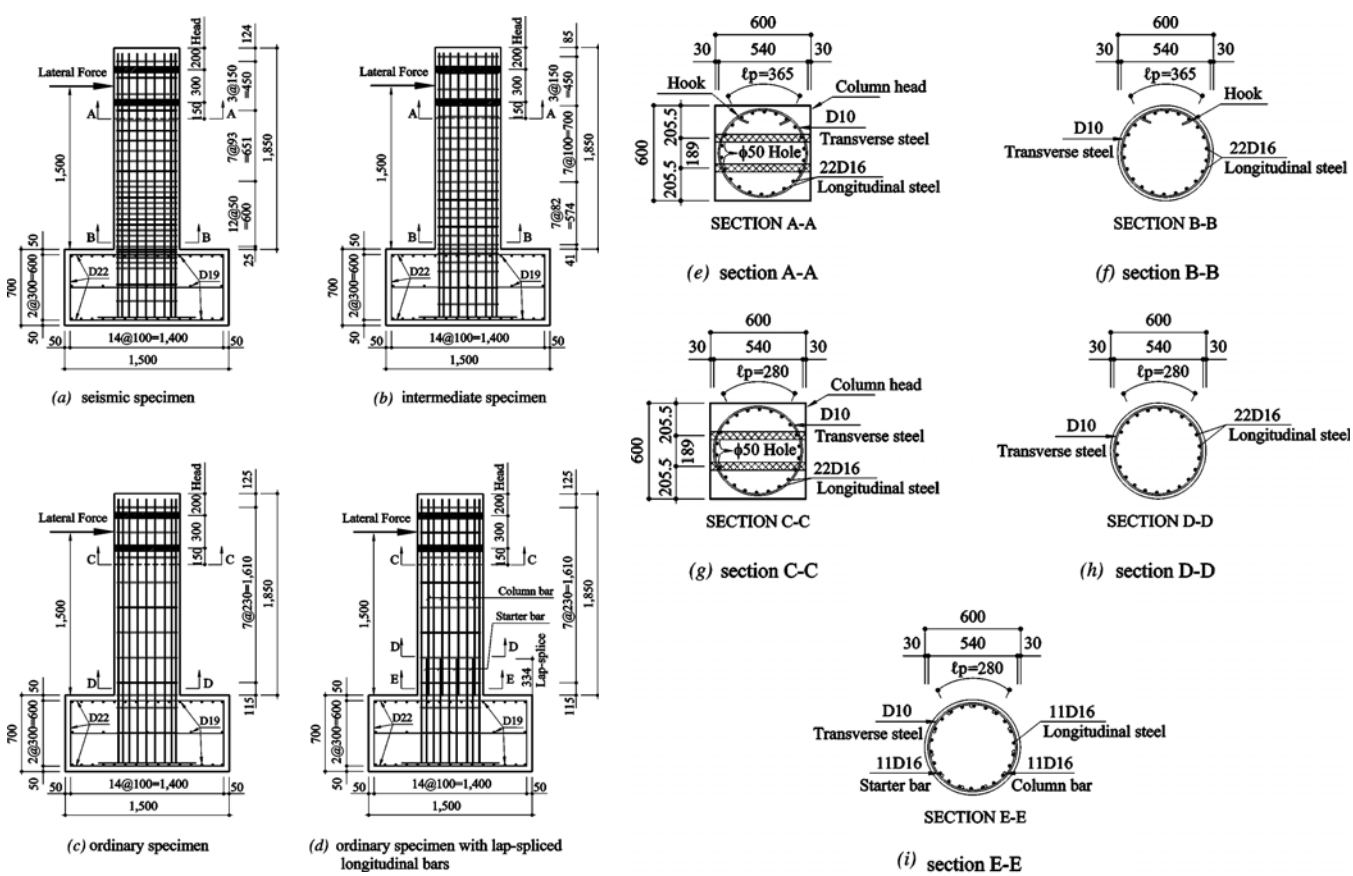

Fig. 1—Details of test specimens. (Note: units in mm; 1 mm = 0.0394 in.)

in 1992. The knowledge gained from this study is significant for the assessment of the seismic reliability of damaged bridge piers and how to repair and strengthen them after they have been damaged in preceding earthquakes.

TEST PROGRAM

Test specimens

Eight circular test columns 600 mm (23.6 in.) in diameter and 1500 mm (59.0 in.) in height were constructed at a scale of 2.5 (refer to Fig. 1). Four test specimens (DN-SP05-R0, DN-SP05-RA, DN-SP05-RC, and DN-SP05-RG [refer to Table 1]) were constructed using starter bars that were lapped with 50% of the longitudinal reinforcement. As shown in Fig. 2, the remaining longitudinal reinforcing bars were extended into the footing. The starter bars were lapped with the main longitudinal reinforcement over a length of 334 mm (13.1 in.). This length was obtained based on the expression $0.007f_y d_b$ of the pre-1992 KHBDS for compression reinforcement, which was derived from the AASHTO expression $0.073\ f_y d_b$. D16 deformed bars were used as longitudinal reinforcement and D10 deformed bars for lateral reinforcement. As shown in Fig. 1(e) through (i), the lateral reinforcement for the ordinary test specimens was closed without hooks, whereas those for intermediate and seismic test specimens were closed with 135-degree hooks on both ends. The yield strengths were determined from tensile coupons as 367 MPa (53.3 psi) for D16 deformed bars and 357 MPa (51.8 psi) for D10 deformed bars. The concrete compressive strength f_c' was 27 MPa (3.9 psi). The maximum aggregate size was 25 mm (1.0 in.). As shown in Fig. 1, ordinary test Specimen DN-SP00-R0 was designed on the basis of the pre-1992 design code of KHBDS. Test Specimens DL-SP00-R0 and US-SP00-R0 were designed in accordance with the limited ductile and full ductile concepts, respectively, and therefore referred to as intermediate. Specimens UN-SP00-R0 and US-SP00-R0 were not subjected to damage-inducing earthquakes before QST, unlike the other specimens. Table 1 shows further details of all test specimens.

Retrofit scheme

Fiber-reinforced composites have long been recognized for their high strength, good fatigue life, light weight, ease of transportation and handling, and low maintenance costs. Fiber composites are generally constructed of filaments, such as glass, aramid, and carbon, embedded in a resin matrix. Fibers are the primary load-carrying elements within the composite. The matrix binds the fibers together and transfers loads between them. Fibers strongly influence the mechanical properties of the composite, such as strength, elastic modulus, and deformation. The stress-strain relationship of a typical composite strap is linear-elastic up to failure. Mechanical properties of the fiber composite straps used herein are listed in Table 2.

The three Specimens DN-SP50-RA, DN-SP50-RC, and DN-SP50-RG were strengthened using aramid, carbon, and glass materials straps, with tensile strengths of 2058, 3479, and 549 MPa (298.4, 504.5, and 79.6 psi), respectively. The required fiber sheet thickness can be calculated by Eq. (1) of Priestley et al.[9] and Eq. (2) and (3) of Seible et al.[10]

$$t_j = \frac{0.1(\varepsilon_{cu} - 0.004)Df_{cc}'}{f_{uj}\varepsilon_{uj}} \tag{1}$$

$$t_j = \frac{0.09(\varepsilon_{cu} - 0.004)Df_{cc}'}{\phi_f f_{uj}\varepsilon_{uj}} \tag{2}$$

$$t_j = 500\frac{D(f_\ell - f_h)}{E_j} \tag{3}$$

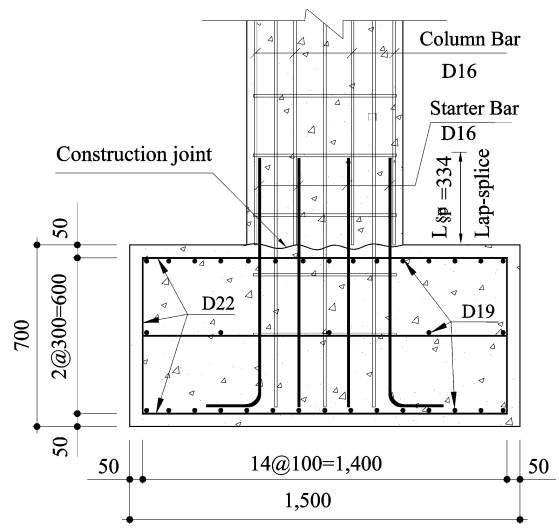

Fig. 2—Lap splice details of longitudinal bars. (Note: units in mm; 1 mm = 0.0394 in.)

Table 1—Characteristics of test specimen

Design concept	Nomenclature*	Longitudinal steel		Confinement steel		FRP thickness, mm	Axial force, kN
		Ratio, %	Lap splice, %	Ratio, %	Spacing, mm WPHR/OPHR†		
Ordinary	UN-SP00-R0	22D16 1.55	0	0.23	230/230	None	$0.1f_c'A_g$ = 664.4
	DN-SP00-R0						
	DN-SP50-R0		50				
	DN-SP50-RG					2.600	
	DN-SP50-RA					0.386	
	DN-SP50-RC					0.334	
Intermediate	DL-SP00-R0		0	0.86	82/100	None	
Seismic	US-SP00-R0			1.31	50/93	None	

*UN = undamaged ordinary design specimen; DN = damaged ordinary design specimen; DL = damaged intermediate design specimen; US = undamaged seismic design specimen; SP = lap splice, R = retrofit; G = glass; A = aramid; and C = carbon.
†WPHR = within plastic hinge region; and OPHR = outside plastic hinge region.
Note: 1 mm = 0.0394 in.; 1 MPa = 145 psi; and 1 kN = 0.225 kip-force.

where t_j is the fiber sheet thickness; ε_{cu} and ε_{uj} are the ultimate strain of confined concrete and fiber sheet, respectively; D is the test specimen diameter; f_{cc}' and f_{uj} are the maximum strength of confined concrete and fiber sheets, respectively; ϕ_f is the flexural capacity reduction factor; f_t is the lateral clamping pressure; and f_h is the horizontal stress level provided by existing hoop reinforcement in a circular column at a strain of 1000 $\mu\varepsilon$.

It is noted that Eq. (1) and (2) are identical when the flexural capacity reduction factor ϕ_f is taken as 0.9, and Eq. (3) is suggested for the retrofit of RC bridge piers only with 100% of the longitudinal reinforcement lap-spliced. Chung et al.,[11,12] however, reported that though a column with 50% of the longitudinal reinforcement spliced was retrofitted as of Eq. (1), it exhibited similar performance as a seismically designed column. Thus, in the present study, Eq. (1) was used for the retrofit of specimens with 50% of the longitudinal reinforcements lap-spliced. Required thicknesses of glass, carbon, and aramid fiber-reinforced straps were computed as shown in Table 2. Considering the standard thicknesses of commercial fiber sheets and the expected flexural-shear failure mode of ordinary specimens, two layers of fiber sheets were used for the retrofit of the three ordinary specimens with lap-spliced longitudinal reinforcement. Anticipating a flexure shear failure mode of ordinary specimens with 50% longitudinal bars lap-spliced, they were wrapped 750 mm (29.5 in.) above the top of the footing. After the straps were wrapped around the columns, epoxy was applied to the surface of the straps and multiple layers of the straps were adhered together to form a single composite wrap of the desired thickness. The ductilities of the retrofitted specimens were greater than the demand ductility.

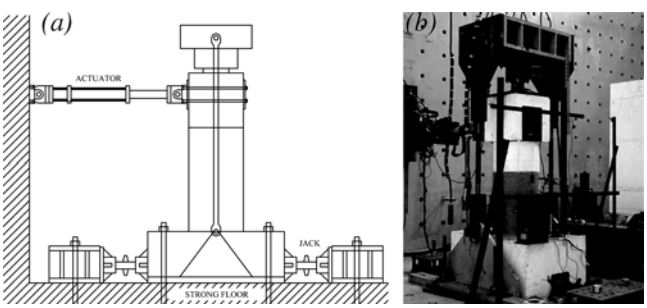

Fig. 3—Test setup.

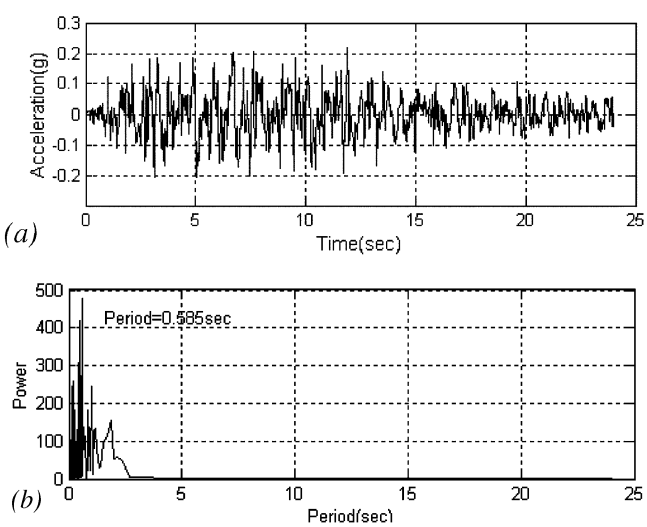

Fig. 4—Input earthquake motions of PDT: (a) ground motions in time domain; and (b) power spectrum of ground motions.

Test setup and instrumentation

Because all test columns were cantilevers, the test setup was designed for testing column-footing assemblages subjected to a combination of axial and lateral loadings. These two loads were applied independently. As shown in Fig. 3, the constant axial load of 664.4 kN (149.4 kip) calculated from the equation $P/f_cA_g = 0.1$, was applied to the top surface of the column by stressing a pair of high-strength steel rods against the reinforced strong floor via a loading frame. Cyclic lateral loads were applied by a 1000 kN (224.8 kip) hydraulic actuator mounted on the reaction wall. Each test column was instrumented to monitor displacements and their corresponding loads, strains, and deformations. These measurements were obtained using: (a) calibrated load cell and displacement transducer of the actuator; (b) clip gauges and inclinometers mounted on the plastic hinge region of the column to measure curvature; (c) displacement transducers installed on the reference frame; and (d) electrical-resistance strain gauges bonded to reinforcing bars.

Loading pattern

The experimental program consisted of two parts: the PDT to induce damage that can be expected from seismic ground motions on the Korean peninsula (Fig. 4) and the subsequent QST to evaluate and enhance the residual seismic performance of earthquake-damaged RC bridge piers. Six test columns were pseudo-dynamically loaded and damaged by four artificial earthquake motions with different PGA values, according to the seismic design provision of KHBDS. The peak ground accelerations of the four input ground motions were 0.0803g, 0.11g, 0.154g, and 0.22g, which correspond to 200-, 500-, 1000-, and 2000-year return periods, respectively. The PDT involves a series of standard step-by-step linear analyses using Newmark's explicit β-method. As can be seen in Fig. 4(b), the dominant period of the input ground motion was 0.585 seconds.

Directly following the PDT, the QST was carried out under displacement control. As shown in Fig. 5, load was applied in the form of a drift ratio, starting with ±0.25%, and increased to ±0.5, ±1.0, ±1.5, ±2.0, ±2.5, ±3.0, ±4.0%, etc., up to failure. The drift level was computed as the ratio of input displacement to column height.

TEST RESULTS AND DISCUSSION

Load-displacement response

Pseudo-dynamic test—All test specimens exhibited cracks concentrated within the plastic hinge regions. The first

Table 2—Mechanical properties of fiber-reinforced polymer composite straps

Fiber	Tensile strength, MPa	Tensile modulus, MPa	Elongation, %	Unit thickness, mm	Required thickness, mm	
					Eq. (1)	Eq. (3)
Glass	571	25,714	2.0	1.3	1.12	17.68
Aramid	2143	112,244	2.6	0.193	0.231	4.05
Carbon	3622	239,796	1.5	0.167	0.236	1.90

Note: 1 mm = 0.0394 in.; and 1 MPa = 145 psi.

earthquake with a PGA of 0.0803g produced initial flexural cracks that were distributed over the height of 370 and 400 mm (14.5 to 15.75 in.) above the footing. Because the maximum displacements of Fig. 6 were less than corresponding yield displacements (Table 3) after completion of the PDT, all test specimens appeared to behave elastically. Many hairline cracks, however, were observed in the plastic hinge region. Concrete cracks could not be observed in the retrofitted specimens because they would be covered by the fiber sheets. As shown in Fig. 6, Specimens DN-SP00-R0 and DL-SP00-R0, without lap splice, behaved almost linearly up to the earthquake motion with a PGA of 0.22g, regardless of different lateral confinement. Similarly, the three retrofitted specimens, DN-SP50-RG, DN-SP50-RA, and DN-SP50-RC, exhibited near-linear elastic behavior.

Quasi-static test—Most specimens failed due to buckling or fracture of longitudinal reinforcement, except for Specimens UN-SP00-R0 and DN-SP00-R0, which failed in shear, without fracture of longitudinal reinforcing bars.

Specimen UN-SP00-R0 developed an initial flexural crack at 0.25% drift, and the cold joint between column and footing cracked at 0.5% drift. Longitudinal cracks appeared at 2.0% drift, and the cover concrete spalled off at 2.5% drift. At 4.0% drift, significant diagonal cracks occurred, which caused a rapid reduction of the column's load-carrying capacity.

Specimen DN-SP00-R0 developed longitudinal cracks at 1.5% drift, that is, earlier than the 2% drift for Specimen UN-SP00-R0. At 5.0% drift, significant diagonal cracks were observed that caused the column to fail without fracture of longitudinal bars. The failure was typical of a flexure-shear failure mode. As shown in Fig. 7(a) and (b), however, the seismic performance of ordinary Specimen DN-SP00-R0 with the predamage was slightly less than that of ordinary Specimen UN-SP00-R0 without the predamage. In Specimen DN-SP50-R0 with a lap splice, the cover concrete spalled off at 3.0% drift, and the member failed at 5.0% drift in the lap splice by fracturing of the longitudinal steel. Specimen DL-SP00-R0, designed for limited seismic exposure, showed more ductile behavior, with initial fracture of longitudinal steel occurring at 7.0% drift.

In the three retrofitted Specimens DN-SP50-RA, DN-SP50-RC, and DN-SP50-RG, the fiber sheets tore off at 5.0% drift. In these specimens, retrofitted with glass, aramid, carbon fiber sheets, fracture of longitudinal steel occurred at 6.0%, 7.0%, and 7.0% drift, respectively.

Specimen US-SP00-R0 had an initial failure pattern similar to Specimen DL-SP00-R0. Beyond 6.0% drift, longitudinal bars began to fracture, and the specimen failed at 7.0% drift. Most specimens failed in flexure, except for Specimens UN-SP00-R0 and DN-SP00-R0, which showed a flexure-shear failure mode.

The hysteresis behaviors of all eight test specimens during the quasi-static test are shown in Fig. 7(a) to (h). According to Fig. 7(a) and (b), undamaged test Specimen UN-SP00-R0 had a higher lateral load capacity (up to 3.0% drift) than damaged test Specimen DN-SP00-R0. The lateral load-carrying capacity of both specimens decreased suddenly due to shear failure at 4.0 and 6.0% drift, respectively. The three retrofitted specimens developed higher lateral forces than the reference Specimen DN-SP50-R0 without retrofit. As shown in Fig. 7(b) and (c), the ordinary test Specimen DN-SP00-R0 without lap splices survived more ductile hysteresis loops than the ordinary test Specimen DN-SP50-R0 with lap splices. As can be seen in Fig. 7(c) to (f), fiber sheets increased the displacement ductility remarkably. According to Fig. 7(a), (b), (g), and (h), the displacement ductility increased as the spacing of lateral reinforcement decreased. Seismic Specimen US-SP00-R0 exhibited the most stable behavior and energy absorption capacity of all specimens.

Displacement ductility

In Fig. 8(a) to (d), the envelopes of the lateral force-displacement responses of all test specimens are compared with allow an assessment of the effects of prior damage, transverse confinement, lap splice, and retrofit measures. Predamaged Specimen DN-SP00-R0 developed lower yield and maximum lateral loads than undamaged Specimen UN-SP00-R0, but a 15% larger ultimate displacement (Fig. 8(a)). As expected, Fig. 8(b) confirms that closer spaced lateral confinement reinforcement in the plastic hinge region increases the ductility.

According to Table 3, the ultimate displacement of seismic Specimen US-SP00-R0 was 1.91 times as large as that of the ordinary Specimen UN-SP00-R0, whereas that of intermediate Specimen DL-SP00-R0 was 1.39 times that of Specimen DN-SP00-R0.

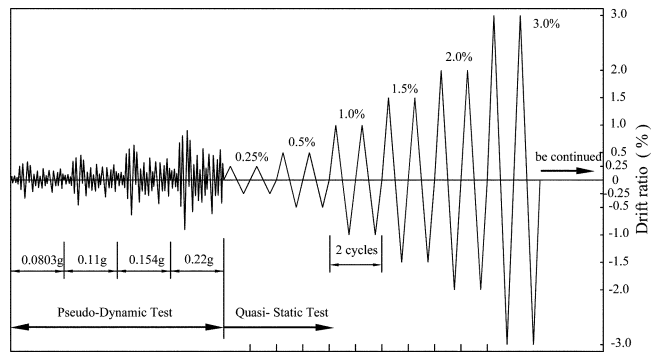

Fig. 5—Load histories of PDT and QST.

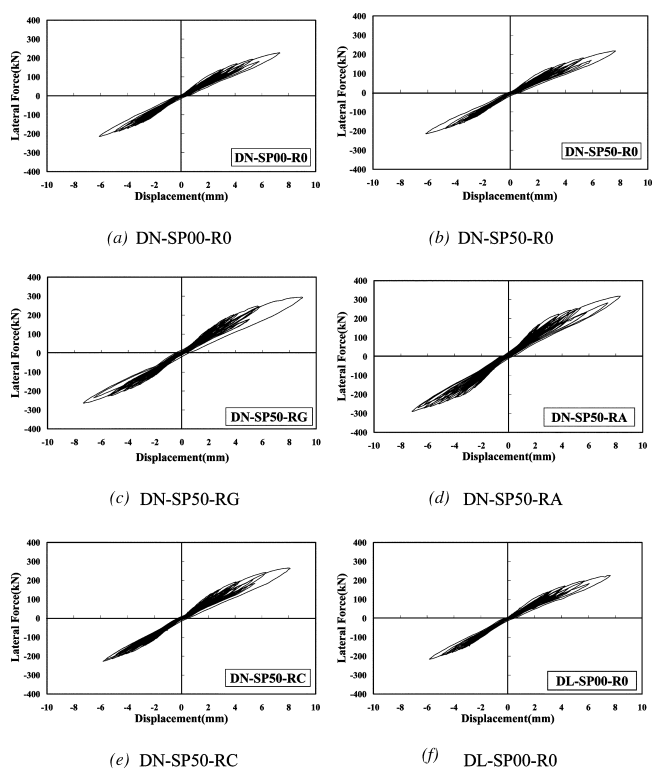

(a) DN-SP00-R0 *(b)* DN-SP50-R0 *(c)* DN-SP50-RG *(d)* DN-SP50-RA *(e)* DN-SP50-RC *(f)* DL-SP00-R0

Fig. 6—Lateral force-displacement response during PDT. (Note: 1 mm = 0.0394 in.; 1 kN = 0.225 kip-force.)

Lap splicing of longitudinal bars in test Specimen DN-SP50-R0 reduced the displacement ductility considerably (Fig. 8(c)). That specimen also lost strength rapidly, whereas Specimen DN-SP00-R0, without a lap splice, showed only a gradual decrease in lateral strength. Figure 8(d) illustrates the effect of FRP retrofitting, which increases the strength and displacement ductility of retrofitted columns with lap splices considerably, to be comparable with those of intermediate Specimen DL-SP00-R0.

To minimize major damage and ensure the survival of structures with moderate lateral load resistance, they must be capable of sustaining their initial strength when a major earthquake imposes large deformations. The lateral displacement is the most convenient quantity to evaluate both the structure's ductility capacity and the demand of an

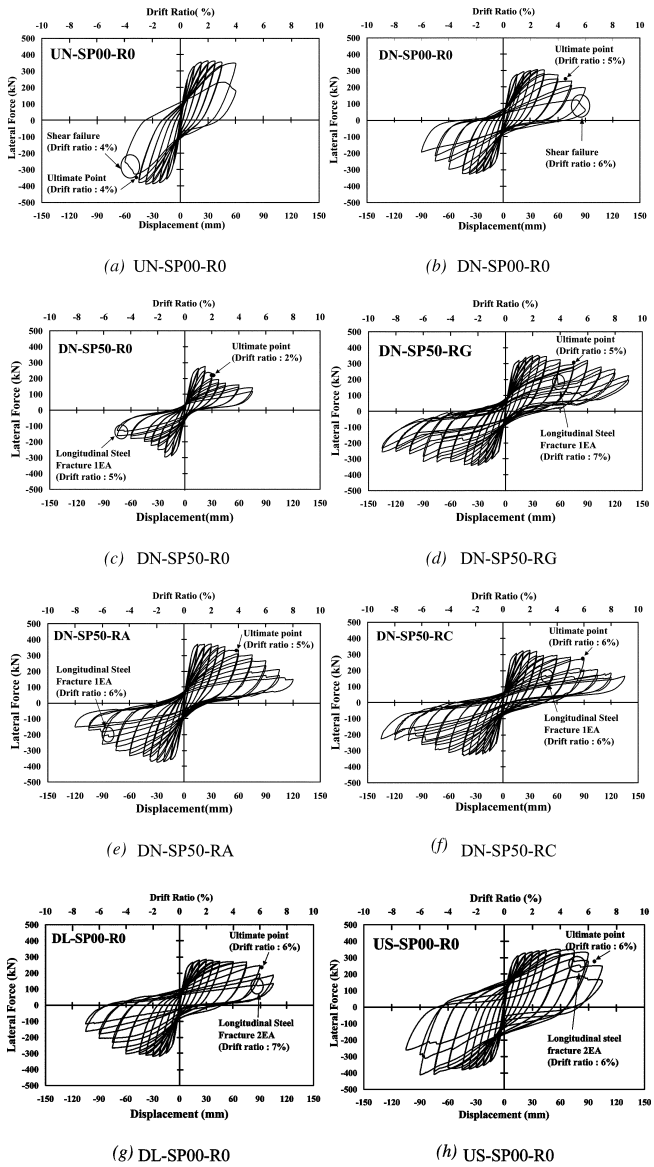

Fig. 7—Lateral force-displacement response during QST. (Note: 1 mm = 0.0394 in.; 1 kN = 0.225 kip-force.)

Table 3—Displacement ductilities

Specimen	Yield		Ultimate		Displacement ductility
	Force, kN	Displacement, mm	Force, kN	Displacement, mm	
UN-SP00-R0	307.1	11.60	330.6	49.71	4.28
DN-SP00-R0	265.8	10.82	265.7	66.00	6.10
DN-SP50-R0	241.8	9.82	300.0	24.08	2.45
DN-SP50-RA	343.5	9.50	322.2	70.00	7.37
DN-SP50-RG	309.1	11.19	305.6	74.93	6.70
DN-SP50-RC	289.4	10.65	282.1	88.00	8.26
DL-SP00-R0	248.1	10.13	245.1	92.00	9.08
US-SP00-R0	292.2	11.38	298.2	95.10	8.36

Note: 1 mm = 0.0394 in.; and 1 kN = 0.225 kip-force.

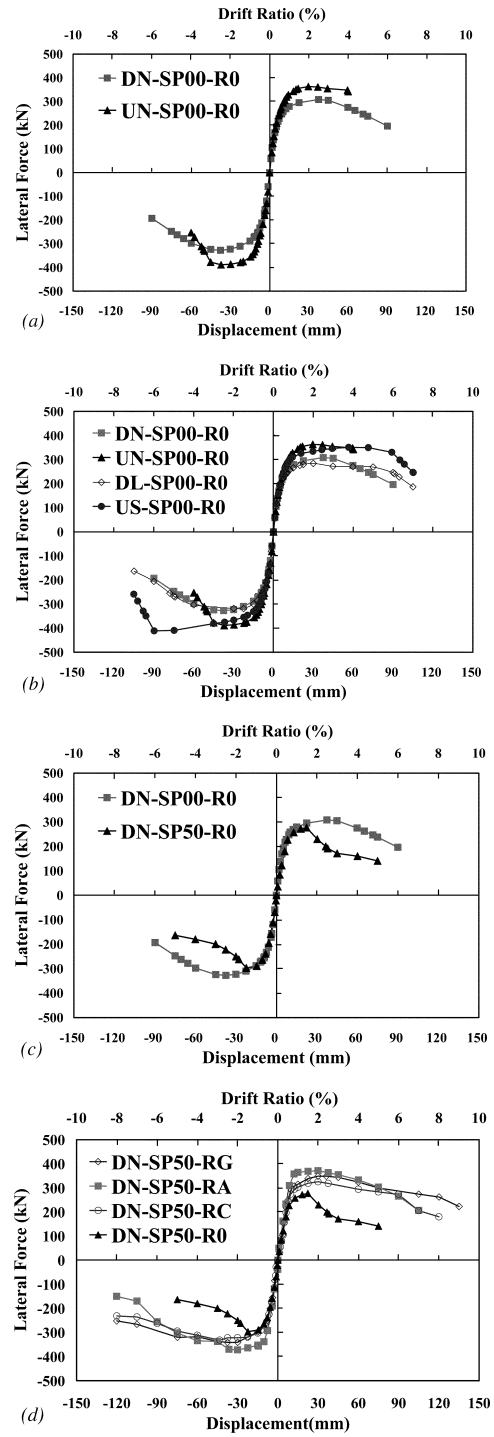

Fig. 8—Lateral force-displacement response envelopes: (a) earthquake predamage; (b) lateral confinement; (c) lap splice; and (d) retrofit. (Note: 1 mm = 0.0394 in.; 1 kN = 0.225 kip-force.)

earthquake. The ultimate displacement Δ_u is defined as the smaller of the maximum experienced when the longitudinal or confinement steel fails and the displacement at which the strength on the descending branch of the force-displacement envelope curve becomes less than $0.85V_{max}$. The yield displacement is defined as the displacement of the intersection point of the following two lines: the straight line that passes through the origin and $0.75V_{max}$ of the envelope curve, and the line that passes V_{max} on the envelope curve and is horizontal to the x-axis.

Results of displacement ductility $\mu = \Delta_u/\Delta_y$ are listed in Table 3. The retrofit increased this ductility for Specimens DN-SP50-RG, DN-SP50-RA, and DN-SP50-RC by factors of 2.7 to 3.4 compared with reference test Specimen DN-SP50-R0, whereas lap splice of Specimen DN-SP50-R0 reduced it to approximately 0.4 times that of reference Specimen DN-SP00-R0. Damaged Specimen DN-SP00-R0 exhibited a larger displacement ductility than undamaged Specimen UN-SP00-R0. The lower displacement ductilities of Specimens DN-SP00-R0 and UN-SP00-R0 are a result of the shear failures of these specimens.

Curvature ductility

The most common and desirable source of inelastic member deformation is the rotation within the plastic hinge region. Therefore, it is useful to relate the rotation per unit length, that is, the curvature, to the corresponding bending moment. This relationship is shown in Fig. 9 for the plastic hinge regions of all specimens subjected to quasi-static cyclic loads. These moment-curvature hysteresis curves have similar shapes as the force-displacement hysteresis curves of Fig. 7. The seismic performance of Specimen DN-SP50-R0 was determined to be very poor because of the lap-splice of 50% longitudinal steel and insufficient lateral reinforcement. In contrast, three retrofitted Specimens DN-SP50-RA, DN-SP50-RG, and DN-SP50-RC showed good ductilities and strength capacities (Fig. 9(c) to (f)). Also, lateral confinement of the plastic hinge region improves the curvature ductility, as seen in Fig. 9(b), (g), and (h). Compared with the ultimate curvature of ordinary Specimen DN-SP00-R0, those of intermediate Specimen DL-SP00-R0 and seismic Specimen US-SP00-R0 were 60.6 and 62.6% larger, respectively.

The envelopes of the moment curvature hysteresis plots are given in Fig. 10 for all eight specimens. The curvature ductility ratio is defined similarly as the displacement ductility, namely, $\mu_\phi = \phi_u/\phi_y$, where ϕ_u is the ultimate curvature and the yield curvature. The yield and ultimate curvatures are similarly defined as the ultimate and yield displacements.

According to Table 4, the lap splice of Specimen DN-SP50-R0 reduced the curvature ductility to approximately 50% of that of nonspliced Specimen DN-SP00-R0, whereas the retrofit measures in Specimens DN-SP50-RG, DN-SP50-RA, and DN-SP50-RC increased the corresponding ductilities by factor 3 to 4, compared with that of Specimen DN-SP50-R0 without retrofit, and these were similar to that of intermediate Specimen DL-SP00-R0, which was twice that of ordinary Specimen DN-SP00-R0. The ductility of even the column with lap-spliced longitudinal reinforcing bars can be increased significantly if retrofitted with FRP wraps.

The curvature ductility capacity of intermediate Specimen DL-SP00-R0 was determined as 15.81, or twice the demand of 7 required for the limited ductile concept of Eurocode 8, and higher than the demand of 13 required by that code for the ductile concept. Ordinary Specimen DN-SP00-R0 without a lap splice of longitudinal steel provided the curvature ductility capacity called for by the limited ductile concept of Eurocode 8, whereas lap-spliced ordinary Specimen DN-SP50-R0 did not. Also, the curvature ductility of seismic Specimen DS-SP00-R0 was determined to be much higher than the demand of 13 that Eurocode 8 requires for the ductile concept.

Energy absorption capacity

Figure 11 shows the cumulative energy absorption capacities of all test specimens. The energies absorbed in each load

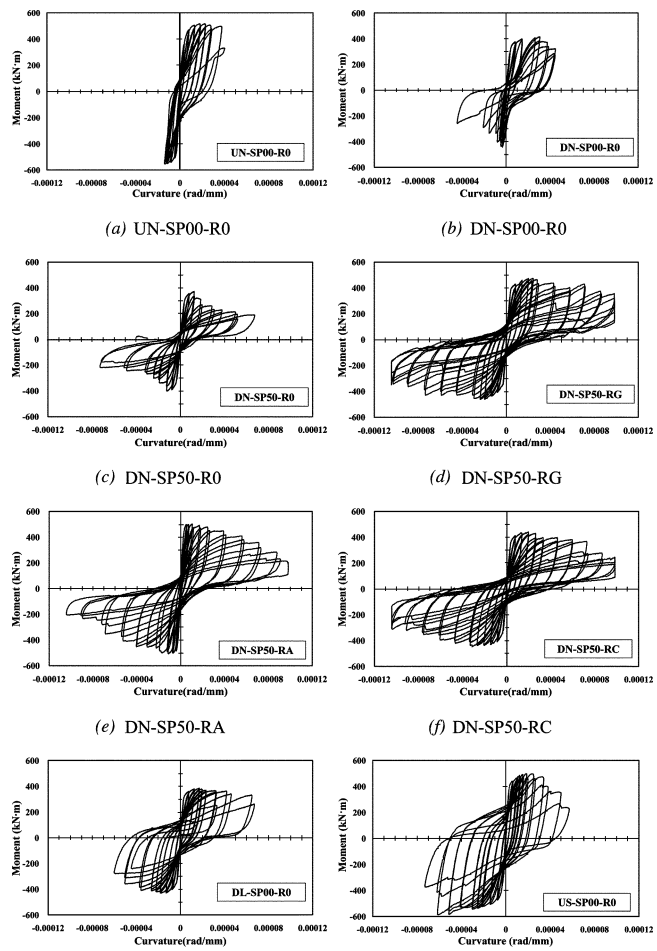

(a) UN-SP00-R0 (b) DN-SP00-R0 (c) DN-SP50-R0 (d) DN-SP50-RG (e) DN-SP50-RA (f) DN-SP50-RC (g) DL-SP00-R0 (h) US-SP00-R0

Fig. 9—Moment-curvature responses. (Note: 1 mm = 0.0394 in.; and 1 kN = 0.225 kip-force.)

Table 4—Curvature ductilities

Specimen	Yield		Ultimate		Curvature ductility
	Moment, kN·m	Curvature, rad/mm	Moment, kN·m	Curvature, rad/mm	
UN-SP00-R0	428.1	5.58E-6	439.1	3.85E-5	6.90
DN-SP00-R0	345.6	5.18E-6	351.1	4.06E-5	7.82
DN-SP50-R0	306.4	4.24E-6	316.7	1.78E-5	4.22
DN-SP50-RA	446.8	3.80E-6	424.6	5.00E-5	13.16
DN-SP50-RG	394.2	4.42E-6	461.7	5.86E-5	13.27
DN-SP50-RC	373.9	4.36E-6	372.9	6.74E-5	15.47
DL-SP00-R0	326.7	4.12E-6	324.0	6.52E-5	15.81
US-SP00-R0	465.9	3.66E-6	498.7	6.60E-5	18.01

Note: 1 mm = 0.0394 in.; and 1 kN = 0.225 kip-force.

cycle were calculated from the hysteresis loop. As shown in Fig. 11(a), undamaged Specimen UN-SP00-R0 absorbed 75% more energy at 4% drift before shear failure than damaged Specimen DN-SP50-R0. Figure 11(b) illustrates the benefit of lateral confinement reinforcement in the plastic hinge region. Lap splicing 50% of the longitudinal reinforcement bars reduced the energy absorption capacity by approximately 50% (compare Specimens DN-SP5O-R0 and DN-SP00-R0 [Fig. 11(c)]), whereas retrofitting increased it by more than 210% (compare Specimens DN-SP50-RA, DN-SP50-RC, and DN-SP50-RG with nonretrofitted test Specimen DN-SP50-R0 [Fig. 11(d)]).

CONCLUSIONS

Test results showed that RC bridge piers damaged during a series of probable earthquake ground motions of the pseudo-dynamic test retain good residual seismic resistance and that retrofitting them with fiber composite wraps in the potential plastic hinge region is an effective way of enhancing their flexural ductility even for a flexural shear failure mode. Lap-spliced RC piers are especially vulnerable and need to be retrofitted to secure good seismic performance in subsequent earthquakes. The eight scale-model tests of RC bridge piers reported herein permit to draw the following conclusions:

1. During earthquake motions with 0.22g PGA in a PDT, all test specimens behaved almost linear elastically with minor damage;

2. Ordinary RC bridge piers with lap-spliced longitudinal reinforcement in the plastic hinge region, that is, without regard for seismic design provisions, exhibited much lower displacement and curvature ductilities than those without such splices;

3. Retrofitting measures considerably increased the lateral strength and ductility of test specimens to values comparable with those of specimens designed for limited seismic response;

4. Because the Korean peninsula is considered to be a low or moderate seismic region, RC bridge piers now in service, which were constructed with 50% of the longitudinal reinforcing reinforcement spliced, in accordance with the pre-1992 design code, can satisfy the seismic requirements of the KHBDS if they are appropriately retrofitted with FRP wraps; and

5. It is especially noted that in the case of retrofit of columns with 50% of the longitudinal bars spliced, Eq. (1) is

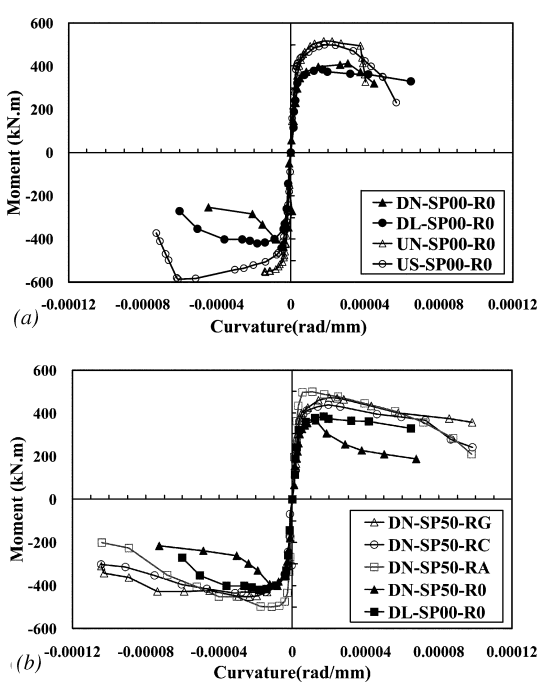

Fig. 10—Moment-curvature response envelopes: (a) transverse confinement; and (b) retrofit. (Note: 1 mm = 0.0394 in.; 1 kN = 0.225 kip-force.)

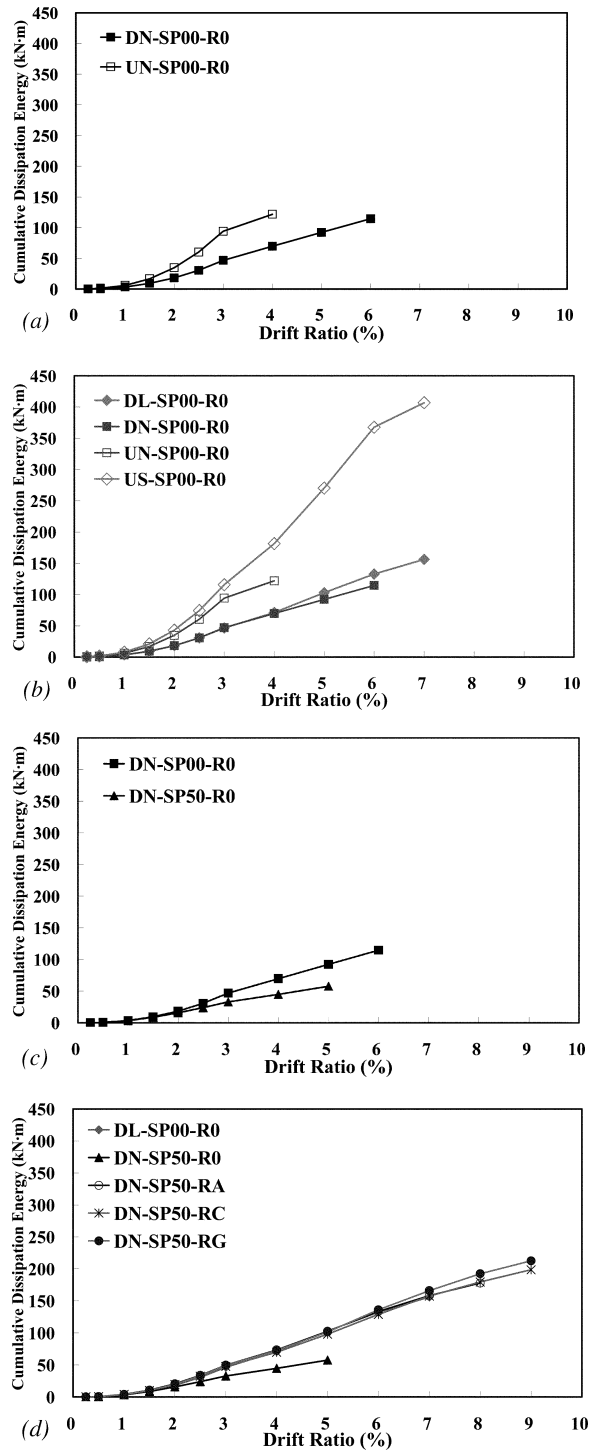

Fig. 11—Cumulative energy absorption versus drift ratio: (a) earthquake predamage; (b) lateral confinement; (c) lap splice; and (d) retrofit. (Note: 1 mm = 0.0394 in.; 1 kN = 0.225 kip-force.)

more appropriate than Eq. (3) to determine the required fiber sheet thickness, because the latter equation was derived for a column with 100% the longitudinal bars spliced.

ACKNOWLEDGMENTS

The authors gratefully acknowledge the support from the Infra-Structures Assessment Research Center (ISARC) funded by Korea Ministry of Construction and Transportation (MOCT).

NOTATION

A_g	=	gross sectional area
b_d	=	bar diameter
D	=	specimen diameter
f_c'	=	concrete compressive strength
f_{cc}'	=	maximum strength of confined concrete
f_{uj}	=	maximum strength of fiber sheet
f_y	=	yield strength of reinforcing bar
$P/f_c'A_g$	=	axial force ratio
t_j	=	thickness of fiber sheet
Δ_u	=	ultimate displacement under quasi-static loading
Δ_y	=	yield displacement
ε_{cu}	=	ultimate strain of confined concrete
ε_{uj}	=	ultimate strain of fiber sheet
ϕ_u	=	ultimate curvature
ϕ_y	=	yield curvature
μ_Δ $(=\Delta_u/\Delta_y)$	=	displacement ductility
μ_ϕ $(=\phi_u/\phi_y)$	=	curvature ductility

REFERENCES

1. Chai, Y.; Priestley, M. J. N.; and Seible, F., "Seismic Retrofit of Circular Bridge Columns for Enhanced Flexural Performance," *ACI Structural Journal*, V. 88, No. 5, Sept.-Oct. 1991, pp. 572-584.

2. Saadatmanesh, H.; Ehsani, M. R.; and Jin, L., "Seismic Strengthening of Circular Bridge Pier Models with Fiber Composites," *ACI Structural Journal*, V. 93, No. 6, Nov.-Dec. 1996, pp. 639-647.

3. Aboutaha, R. S.; Engelhardt, M. D.; Jirsa, J. O.; and Kreger, M. E., "Experimental Investigation of Seismic Repair of Lap Splice Failures in Damaged Concrete Columns," *ACI Structural Journal*, V. 96, No. 2, Mar.-Apr. 1999, pp. 297-307.

4. Lehman, D. E.; Gookin, S. E.; Nacamuli, A. M.; and Moehle, J. P., "Repair of Earthquake-Damaged Bridge Columns," *ACI Structural Journal*, V. 98, No. 2, Mar.-Apr. 2001, pp. 233-242.

5. Ministry of Construction and Transportation, "Korea Highway Bridge Design Specification," Korea Road and Transportation Association, 2000.

6. Einea, A.; Yehia, S.; and Tadros, M. K., "Lap Splices in Confined Concrete," *ACI Structural Journal*, V. 96, No. 6, Nov.-Dec. 1999, pp. 947-955.

7. Jaradat, O. A.; McLean, D. I.; and Marsh, M. L., "Performance of Existing Bridge Columns under Cyclic Loading—Part 1: Experimental Results and Observed Behavior," *ACI Structural Journal*, V. 95, No. 6, Nov.-Dec. 1998, pp. 695-704.

8. Melek, M., and Wallace, J. W., "Cyclic Behavior of Columns with Short Lap Splices," *ACI Structural Journal*, V. 101, No. 6, Nov.-Dec. 2004, pp. 802-811.

9. Priestley, M. J. N.; Seible, F.; and Calvi, G. M., *Seismic Design and Retrofit of Bridges*, John Wiley & Sons Inc., New York, 1996.

10. Seible, F.; Priestley, M. J. N.; Hegemier, G. A.; and Innamorato, D., "Seismic Retrofit of RC Columns with Continuous Carbon Fiber Jackets," *Journal of Composites for Construction*, V. 1, No. 2, 1997, pp. 52-62.

11. Chung, Y. S.; Lee, K. K.; Han, G. H.; and Lee, D. H., "Quasi-Static Test for Seismic Performance of Circular R.C. Bridge Piers Before and After Retrofitting," *Journal of the Korea Concrete Institute*, V. 11, No. 5, 1999, pp. 107-118.

12. Chung, Y. S.; Park, C. K.; and Lee, E. H., "Seismic Performance and Damage Assessment of Reinforced Concrete Bridge Piers with Lap-Spliced Longitudinal Steels," *Structural Engineering and Mechanics*, V. 17, No. 1, 2004, pp. 51-68.